



ELSEVIER

15 January 1999

OPTICS
COMMUNICATIONS

Optics Communications 159 (1999) 266–277

Full length article

Convergence of the T-matrix method for light scattering from a particle on or near a surface

A. Doicu^a, Yu.A. Eremin^b, T. Wriedt^a

^a *Institut für Werkstofftechnik, Badgasteiner Straße 3, 28359 Bremen, Germany*

^b *Department of Applied Mathematics and Computer Science, Moscow State University, Vorobyov Hills, 119899 Moscow, Russia*

Received 7 August 1998; revised 6 October 1998; accepted 27 October 1998

Abstract

Convergence of the T-matrix approach for analyzing the scattering light from a particle located on a smooth surface is investigated. Numerical experiments are performed for oblate spheroids by choosing the discrete source method as reference. The results show that instability and convergence problems occur when the sphere enclosing the singularities of the scattered field intersects the interface. © 1999 Elsevier Science B.V. All rights reserved.

1. Introduction

Particle contamination characterization of a silicon wafer surface is of great importance for semiconductor manufacturing. As semiconductor device dimensions become smaller, there is a need for wafer surface inspection systems to have the capability to detect size of microcontaminations as low as 0.1 μm or even smaller. To expand the current detection ability one must use an efficient mathematical model and computer simulation technique.

Calculation of light scattering from particles deposited on a surface is of great interest in the simulation, development and calibration of a surface scanner. Several studies have addressed this problem using very different methods.

Some simplified theoretical models have been developed on the basis of Mie light-scattering theory and Fresnel surface reflection [1–4]. These approaches represent an extension of the Mie theory and are focussed on the light scattering problem of a sphere on or near a plane surface. A coupled-dipole algorithm has also been employed for the scattering problem [5,6]. In this case an array of dipoles are distributed in a lattice configuration to model its shape and composition. In order to take the presence of unbounded space into account the Sommerfeld integrals for interaction between a dipole and a surface are introduced.

A model based on the discrete source method was given by Eremin et al. [7]. This approach is based on the fact that for a local obstacle deposited near the plane interface it is possible to construct dipoles and multipole fields satisfying the field transmission conditions at this interface. Consequently, all conditions of the scattering problem are analytically satisfied except for the boundary condition at the particle surface. In this case the dipoles and multipole fields are constructed on the basis of the Weyl-Sommerfeld integrals. The Weyl-Sommerfeld integral spectral densities can be obtained by solving one-dimensional transmission problems [7].

In a previous paper we constructed a theoretical model based on the T-matrix approach [8]. The method takes into account that the incident field strikes the particle either directly or after interacting with the surface, while the fields emanating from the particle may also reflect off the surface and interact with the particle again. The reflected scattered field or the interacting field is computed using the integral representation of spherical vector wave functions over plane waves. For these fields we assume expansions in terms of regular or radiating spherical vector wave functions. The transition matrix, or the T-matrix relates the expansion coefficients of the incident fields and the scattered field. However, for some special scattering configurations such an approach is expected to fail as a consequence of the geometrical constraints of the

T-matrix method. The expansion of the scattered field in terms of radiating multipoles is valid outside the circumscribed sphere of the scatterer, and in general this fact generates restrictions in applying the T-matrix method for analyzing multiple scattering problems. For example, in the case of an oblate spheroid situated on a wafer surface the circumscribed sphere intersects the plane interface, and consequently the geometrical constraints of the T-matrix method are violated.

The aim of this paper is to investigate the range of validity of the T-matrix approach by performing numerical experiments for oblate spheroids situated on or near a plane surface. For comparison the discrete source model (based on a strict mathematical model for this scattering problem) is chosen as reference.

2. Mathematical formalism

2.1. Geometry of the scattering problem

The geometry of the scattering system is shown in Fig. 1. An axisymmetric particle is situated on plane surface Σ so that its symmetry axis coincides with the normal to the plane surface. Let us introduce a Cartesian coordinate system $Oxyz$ with the z axis along the symmetry axis of the particle. The origin O is situated at a distance z_0 above the plane surface. The incident radiation is a plane wave traveling in the xz plane, oriented at some angle with respect to the z axis. The wave number in the medium above the surface (ambient medium) is denoted by $k_s = k\sqrt{\epsilon_s\mu_s}$, while the wave vector inside the particle is denoted by $k_t = k\sqrt{\epsilon_t\mu_t}$. Here ϵ_t and μ_t , where $t = s, i$, are the relative permittivity and permeability, respectively.

In the following sections we briefly describe the theoretical models for analyzing the scattering problem of a particle on or near a surface.

2.2. T-matrix method

The incident plane wave strikes the sphere either directly or after interacting with the surface. The field can be expressed as a series of regular spherical vector wave functions (SVWF) $\mathbf{M}_{ml}^1(k_s\mathbf{r})$ and $\mathbf{N}_{ml}^1(k_s\mathbf{r})$, i.e.

$$\mathbf{E}_{\text{inc}}(\mathbf{r}) = \sum_{l=1}^{\infty} \sum_{m=-l}^l D_{ml} [a_{ml}\mathbf{M}_{ml}^1(k_s\mathbf{r}) + b_{ml}\mathbf{N}_{ml}^1(k_s\mathbf{r})]. \tag{1}$$

Here, D_{ml} is a normalization constant and is given by

$$D_{ml} = \frac{2l+1}{4l(l+1)} \frac{(l-|m|)!}{(l+|m|)!}.$$

The expansion coefficients a_{ml} and b_{ml} are separated into two parts

$$a_{ml} = a_{ml}^0 + a_{ml}^R, \quad b_{ml} = b_{ml}^0 + b_{ml}^R, \tag{2}$$

where a_{ml}^0 and b_{ml}^0 correspond to the direct incident field, while a_{ml}^R and b_{ml}^R correspond to the incident field reflected by the plane interface. The expressions for a_{ml}^R and b_{ml}^R contain the Fresnel reflection coefficients and a phase factor arising from the phase difference between the plane wave and its reflected wave in O .

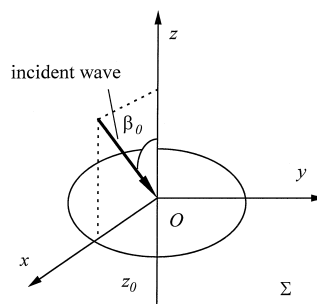


Fig. 1. Geometry of the scattering system.

The scattered field is expressed in terms of radiating SVWF:

$$\mathbf{E}_s^0(\mathbf{r}) = \sum_{n=1}^{\infty} \sum_{m=-n}^n D_{mn} [e_{mn} \mathbf{M}_{mn}^3(k_s \mathbf{r}) + f_{mn} \mathbf{N}_{mn}^3(k_s \mathbf{r})] \tag{3}$$

and this expansion is valid outside a sphere enclosing the scatterer.

In addition to the two fields described by Eqs. (1) and (3), a third field exists in the ambient medium. This field, which for convenience is called the interacting field, is a result of the scattered field reflecting off the surface and striking the particle. The interacting field can be expressed in the following form,

$$\mathbf{E}_s^R(\mathbf{r}) = \sum_{n=1}^{\infty} \sum_{m=-n}^n D_{mn} [e_{mn} \mathbf{M}_{mn}^{3,R}(k_s \mathbf{r}) + f_{mn} \mathbf{N}_{mn}^{3,R}(k_s \mathbf{r})], \tag{4}$$

where $\mathbf{M}_{mn}^{3,R}(k_s \mathbf{r})$ and $\mathbf{N}_{mn}^{3,R}(k_s \mathbf{r})$ denote the radiating SVWF reflected by the surface. For \mathbf{r} inside a sphere enclosed in the particle and a given azimuthal mode m the reflected SVWF are given by:

$$\begin{pmatrix} \mathbf{M}_{mn}^{3,R}(k_s \mathbf{r}) \\ \mathbf{N}_{mn}^{3,R}(k_s \mathbf{r}) \end{pmatrix} = \sum_{l=1}^{\infty} D_{ml} \left[\begin{pmatrix} \alpha_{mnl} \\ \gamma_{mnl} \end{pmatrix} \mathbf{M}_{ml}^1(k_s \mathbf{r}) + \begin{pmatrix} \beta_{mnl} \\ \delta_{mnl} \end{pmatrix} \mathbf{N}_{ml}^1(k_s \mathbf{r}) \right]. \tag{5}$$

Substituting Eq. (5) into Eq. (4) we get a representation of the interacting field in terms of regular SVWF, i.e.

$$\mathbf{E}_s^R(\mathbf{r}) = \sum_{l=1}^{\infty} \sum_{m=-l}^l D_{ml} [e_{ml}^R \mathbf{M}_{ml}^1(k_s \mathbf{r}) + f_{ml}^R \mathbf{N}_{ml}^1(k_s \mathbf{r})], \tag{6}$$

where

$$\begin{pmatrix} e_{ml}^R \\ f_{ml}^R \end{pmatrix} = \sum_{n=1}^{\infty} D_{mn} \left[\begin{pmatrix} \alpha_{mnl} \\ \gamma_{mnl} \end{pmatrix} e_{mn} + \begin{pmatrix} \beta_{mnl} \\ \delta_{mnl} \end{pmatrix} f_{mn} \right]. \tag{7}$$

In the T-matrix method the scattered field coefficients are related to the expansion coefficients of the fields striking the particle by the transition matrix. For an axisymmetric particle the equations become uncoupled, permitting a separate solution for each azimuthal mode. For a fixed azimuthal mode m we truncate the expansions given in Eqs. (1), (3) and (6) and get the following matrix equation for the scattering problem:

$$\begin{bmatrix} e_{mn} \\ f_{mn} \end{bmatrix} = [T_{mnl}] \cdot \left(\begin{bmatrix} a_{ml} \\ b_{ml} \end{bmatrix} + \begin{bmatrix} e_{ml}^R \\ f_{ml}^R \end{bmatrix} \right). \tag{8}$$

Here, $m = \overline{-M, M}$ and $n, l = \overline{1, N}$, where M is the number of azimuthal modes and N is the truncation index. The explicit form of the transition matrix $[T_{mnl}]$ can be found in Refs. [9,10]. The expansion coefficients of the interacting field are related to the scattered field coefficients by a so-called reflection matrix,

$$\begin{bmatrix} e_{ml}^R \\ f_{ml}^R \end{bmatrix} = [A_{mln}] \cdot \begin{bmatrix} e_{mn} \\ f_{mn} \end{bmatrix}, \tag{9}$$

where, accordingly to Eq. (7)

$$[A_{mln}] = \begin{bmatrix} D_{mn} \alpha_{mnl} & D_{mn} \gamma_{mnl} \\ D_{mn} \beta_{mnl} & D_{mn} \delta_{mnl} \end{bmatrix}.$$

The scattered field coefficients e_{mn} and f_{mn} are obtained by combining matrix equations (8) and (9). Explicit expressions for the incident field coefficients a_{ml} and b_{ml} , and the elements of the reflection matrix are given in Ref. [8].

The main steps of the T-matrix approach are summarized as follows:

- calculation of the transition matrix which relates the expansion coefficients of the fields striking the particle to the scattered field coefficients,
- calculation of the reflection matrix characterizing the reflection of SVWF by the surface,
- computation of an approximate solution of the governing matrix equation, and
- extrapolation of the scattered field to the far field.

Let us discuss the validity of the scattered and interacting field expansions. The scattered field representation (3) is valid outside a sphere circumscribing the particle. Since the interacting field \mathbf{E}_s^R is computed from the boundary condition

$$\mathbf{n} \times \mathbf{E}_s^0 + \mathbf{n} \times \mathbf{E}_s^R = \mathbf{n} \times \mathbf{E}_s^T \text{ on } \Sigma$$

assuming that (3) is a valid representation for \mathbf{E}_s^0 , it is clear that the interacting field representation (4) breaks down when the circumscribing sphere intersects the interface.

However, this condition can be relaxed since the boundaries of applicability of representations (3) and (4) are determined by the geometry of the set of singularities associated with the continuation of the wave fields. Let us discuss this subject in detail. The problem of continuation of a solution to a boundary-value problem out of its initial domain of definition comes after a series of failures of computational algorithms. The matter is that working out computational schemes for scattering problems one often has in mind some representation of the solution and the choice of the specific representation determines certain analytic properties of the solution. The computational schemes can be successfully realized only when the existence domain of the chosen analytic representation includes the domain (together with its boundary) in which the solution is searched for. Otherwise the algorithms are unstable and the solution diverges. A solution to the Maxwell equations is a real-analytic function which vanishes at infinity (according to the radiation condition) and, hence, this solution has singularities near the origin. These singularities naturally lie outside the domain where the solution is required or on its boundary. Let us consider a single scatterer and assume that the singularities of the scattered field lie inside a sphere enclosed in the particle. Then expansion (3) allow us to continue the scattered field up to this sphere. This means that the scattered field representation (3) is valid outside a sphere enclosing the singularities of the analytic continuation of the scattered field. Consequently, expansions (3) and (4) are valid if the sphere enclosing the singularities of the scattered field does not intersect the interface.

An equivalent condition can be formulated in the frame of the image theory. The total field scattered from a particle situated on or near a perfectly conducting interface is equivalent to the field scattered from two identical particles which are placed in the original and the image coordinate system [8]. Hence, expansions (3) and (4) are valid representations for the total field $\mathbf{E}_s = \mathbf{E}_s^R + \mathbf{E}_s^0$ if the spheres enclosing the singularities of the scattered field in the real and image spaces do not intersect. Note that for an oblate particle the exact total scattered field $\mathbf{E}_s = \mathbf{E}_s^R + \mathbf{E}_s^0$ has singularities on a disc which contains the interfocal distance and on the image disc with respect to the interface surface.

From a computational point of view the boundaries of applicability of representations (3) and (4) have the following meaning. As the ‘width’ of an oblate spheroid increases the number of terms needed in these expansions increases and the interaction becomes greater and concentrated in higher order terms. Conversely, the matrix equation includes Hankel functions of high order leading to an unstable numerical algorithm and divergent solutions.

2.3. Discrete sources method

Discrete Sources Method (DSM) is a relatively new technique for investigating scattering problems on local obstacles [11]. The essence of the DSM consists in representing the approximate solution of the scattering problem as a finite linear combination of fields of dipoles and multipoles, deposited in a nonphysical region. The amplitudes of the discrete sources (DS) are determined from boundary conditions enforced at the particle surface. Essentially, the scattering problem reduces to the approximation of an exciting field at the particle surface by fields of discrete sources. To provide an estimate of the approximate solution to the exact solution in a uniform metric outside the obstacle it is sufficient to fit the boundary conditions in mean square norm. Completeness of DS fields provides the convergence of the approximate solution to the exact one. The advantage of the DSM consists in the opportunity to estimate the error through the calculation of the residual of the boundary values at the particle surface.

A mathematical statement of the scattering problem under examination includes Maxwell equations anywhere outside the medium discontinuities, transmission conditions at the interface and particle surfaces, and radiation condition at infinity. Prior to constructing an approximate solution for the scattered fields we shall solve the problem of a plane wave scattering at the plane interface. After that we will construct the approximate solution of the scattered field by satisfying explicitly the transmission conditions at the interface. For this purpose we use the Green tensor for a stratified interface, that is

$$\bar{\mathbf{G}}(\mathbf{r}, \mathbf{r}') = \begin{bmatrix} g^{e,h} & 0 & 0 \\ 0 & g^{e,h} & 0 \\ \frac{\partial f}{\partial x} & \frac{\partial f}{\partial y} & \sigma^{e,h} \end{bmatrix} \tag{10}$$

where the tensor elements are given by

$$g^{e,h}(\mathbf{r},\mathbf{r}') = \exp(jk_s R)/R - \exp(jk_s R')/R' + \int_0^\infty J_0(\lambda r) v_{11}^{e,h} \exp[-K_z^0(z+z')] \lambda d\lambda,$$

$$f(\mathbf{r},\mathbf{r}') = \int_0^\infty J_0(\lambda r) v_{31} \exp[-K_z^0(z+z')] \lambda d\lambda,$$

$$\sigma^{e,h}(\mathbf{r},\mathbf{r}') = g^{h,e}(\mathbf{r},\mathbf{r}') \tag{11}$$

Here, $r = [(x-x')^2 + (y-y')^2]^{1/2}$ is the distance on the plane, $R = [r^2 + (z-z')^2]^{1/2}$ is the distance in \mathbf{R}^3 space, R' means $R' = [r^2 + (z+z')^2]^{1/2}$, $K_z^0 = (\lambda^2 - k_r^2)^{1/2}$, and $v_{11}^{e,h}$ and v_{31} are spectral functions providing a fitting of transmis-

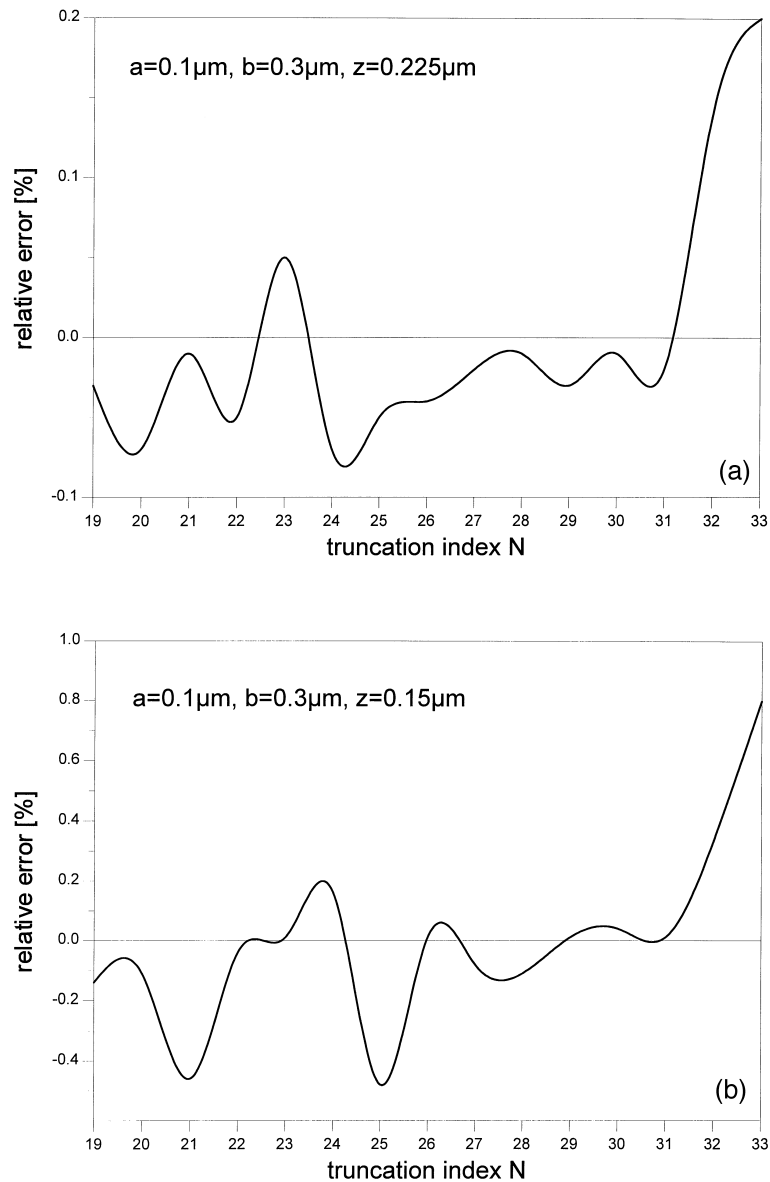


Fig. 2. Relative error of the DSCS at a scattering angle of 0° as a function of the truncation index N . The curves are computed for an oblate spheroid with semiaxes $a = 0.1 \mu\text{m}$ and $b = 0.3 \mu\text{m}$ situated at the distances (a) $z_0 = 0.225 \mu\text{m}$, (b) $z_0 = 0.15 \mu\text{m}$, and (c) $z_0 = 0.1 \mu\text{m}$ above the substrate. The incident light is a p-polarized plane wave having an inclination from the normal of 0° . The relative errors are computed with respect to the mean value of the DSCS over the truncation index N .

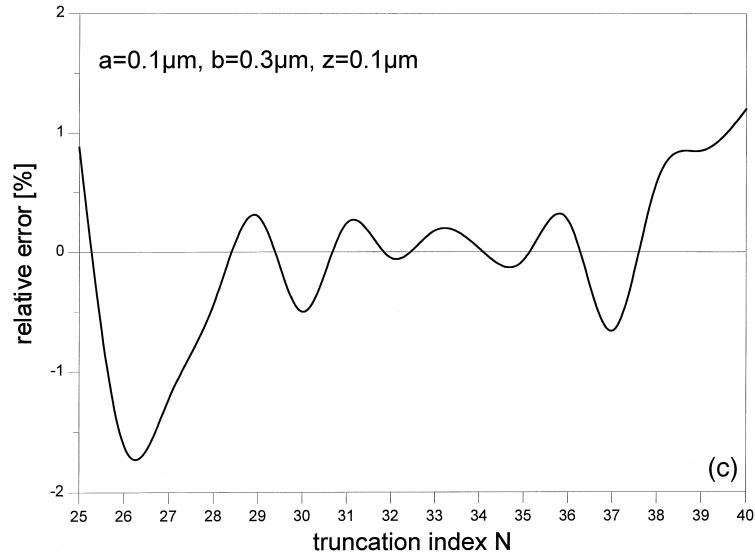


Fig. 2 (continued).

sion conditions at the plane interface explicitly [7]. Denoting the cylindrical coordinates of the observation point \mathbf{r} by (ρ, φ, z) and the cylindrical coordinates of the source point \mathbf{r}' by (ρ', φ', z') , and expanding the components of the Green tensor in Fourier series with respect to the azimuthal variable φ , gives

$$G_{ij}(\mathbf{r}, \mathbf{r}') = \sum_m \Gamma_{ij}^m(\rho, z, \rho', z') \exp[jm(\varphi - \varphi')]. \tag{12}$$

Let us define

$$G_{ij}^m(\rho, z, z') = \lim_{\rho' \rightarrow 0} \left[\frac{\Gamma_{ij}^m(\rho, z, \rho', z')}{\rho'^m} \right]. \tag{13}$$

Then the functions forming the tensor (10) take the following form,

$$g_m^{e,h}(\rho, z, z') = Y_m^s(\rho, z, z') - Y_m^s(\rho, z, -z') + \int_0^\infty J_m(\lambda r) v_{11}^{e,h} \exp[-K_z^0(z+z')] \lambda^{m+1} d\lambda, \tag{14}$$

$$f_m(\rho, z, z') = \int_0^\infty J_m(\lambda r) v_{31} \exp[-K_z^0(z+z')] \lambda^{m+1} d\lambda,$$

where J_m are cylindrical Bessel functions of order m ,

$$Y_m^s(\rho, z, z') = h_m^{(2)} \left(k_s \sqrt{\rho^2 + (z - z')^2} \right) \left(\frac{\rho}{\sqrt{\rho^2 + (z - z')^2}} \right)^m \tag{15}$$

and $h_m^{(2)}$ are spherical Hankel functions.

Let $\{w_n\}_{n=1}^\infty$ be a dense sequence of source points distributed on a segment τ_w of the axis of symmetry Oz , i.e. $w_n \in \tau_w$, where τ_w is located inside the particle. For the field in the ambient medium we define Hertz vectors for vector multipoles by

$$\mathbf{A}_{mnx}^{e,h} = \mathbf{e}_x g_m^{e,h}(\rho, z, w_n) - \mathbf{e}_z f_{m+1}(\rho, z, w_n) \cos \varphi, \tag{16}$$

$$\mathbf{A}_{mny}^{e,h} = \mathbf{e}_y g_m^{e,h}(\rho, z, w_n) - \mathbf{e}_z f_{m+1}(\rho, z, w_n) \sin \varphi,$$

and Hertz vectors for vertical electric dipoles by

$$\mathbf{A}_{0n}^{e,s} = g_0^h(\rho, z, w_n) \mathbf{e}_z. \tag{17}$$

For the field inside the particle we define entire functions with singularities located at infinity by

$$\mathbf{A}_{mnx}^i = \mathbf{e}_x Y_m^i(\rho, z, w_n), \quad \mathbf{A}_{mny}^i = \mathbf{e}_y Y_m^i(\rho, z, w_n) \tag{18}$$

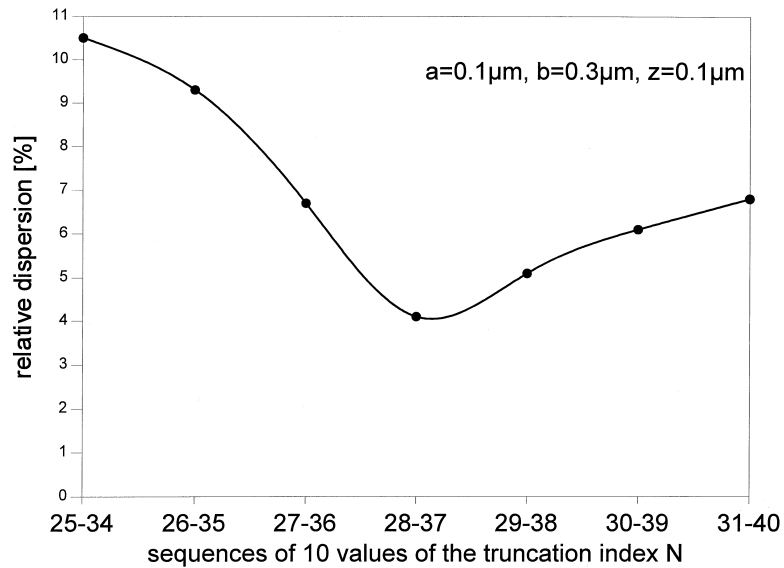


Fig. 3. Relative dispersion σ_r for different sequences of truncation indices for an oblate spheroid with $a = 0.1 \mu\text{m}$ and $b = 0.3 \mu\text{m}$ situated at a distance $z_0 = 0.1 \mu\text{m}$ above the substrate.

and Hertz vectors for vertical electric dipoles by

$$\mathbf{A}_{0n}^{e,i} = Y_0^i(\rho, z, w_n) \mathbf{e}_z. \tag{19}$$

Here,

$$Y_m^i(\rho, z, z') = j_m \left[k_i \sqrt{\rho^2 + (z - z')^2} \right] \left(\frac{\rho}{\sqrt{\rho^2 + (z - z')^2}} \right)^m \tag{20}$$

and j_m are spherical Bessel functions.

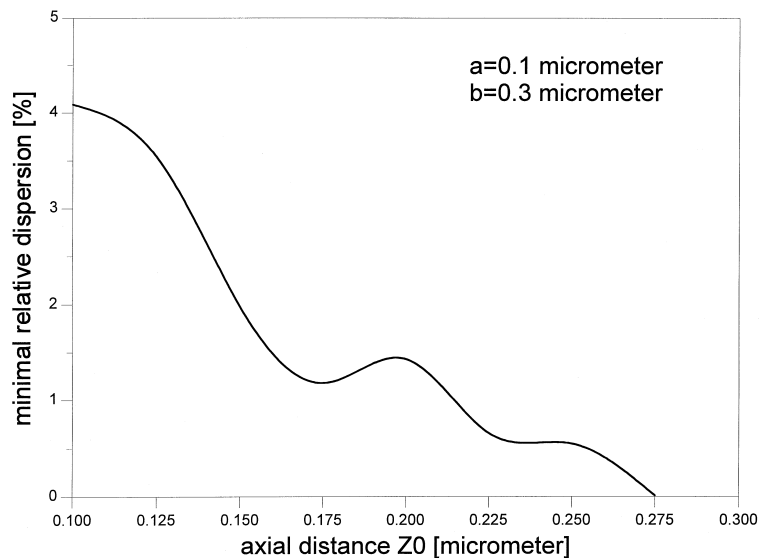


Fig. 4. Minimal relative dispersion σ_r of the differential scattering cross section (DSCS) at a scattering angle of 0° as a function of the axial distance z_0 . The curves are computed for an oblate spheroid with semiaxes $a = 0.1 \mu\text{m}$ and $b = 0.3 \mu\text{m}$. The incident light is a p-polarized plane wave having an inclination from the normal of 0° .

We will construct the approximate solution which takes into account not only the rotational symmetry of the scatter, but simultaneously polarization of the external excitation [7]. Let us consider a P polarized plane wave propagating at some angle with respect to the Oz axis. To represent the total scattered field we use some linear combinations of $\mathbf{A}_{mnx}^{e,h}$ and $\mathbf{A}_{mny}^{e,h}$ to account for the axial symmetry and P polarization of the incident field,

$$\begin{aligned} \mathbf{A}_{mn}^{e,s}(\mathbf{r}) &= \mathbf{A}_{mnx}^e \cos m\varphi - \mathbf{A}_{mny}^e \sin m\varphi, \\ \mathbf{A}_{mn}^{h,s}(\mathbf{r}) &= \mathbf{A}_{mnx}^h \sin m\varphi + \mathbf{A}_{mny}^h \cos m\varphi. \end{aligned} \quad (21)$$

In the same manner we construct the following linear combinations,

$$\begin{aligned} \mathbf{A}_{mn}^{e,i}(\mathbf{r}) &= \mathbf{A}_{mnx}^i \cos m\varphi - \mathbf{A}_{mny}^i \sin m\varphi, \\ \mathbf{A}_{mn}^{h,i}(\mathbf{r}) &= \mathbf{A}_{mnx}^i \sin m\varphi + \mathbf{A}_{mny}^i \cos m\varphi, \end{aligned} \quad (22)$$

to represent the fields inside the particle.

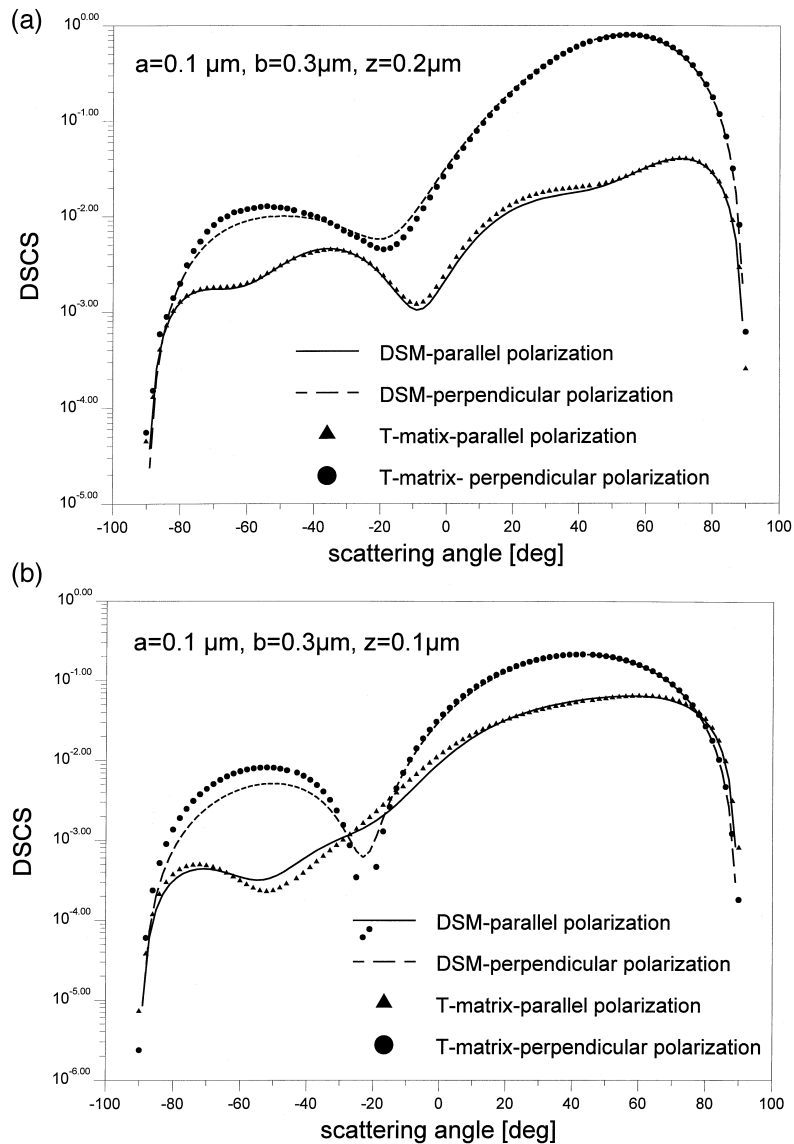


Fig. 5. Differential scattering cross section (DSCS) of an oblate spheroid with semi-axes $a = 0.1 \mu\text{m}$ and $b = 0.3 \mu\text{m}$ situated at a distance: (a) $z_0 = 0.2 \mu\text{m}$ and (b) $z_0 = 0.1 \mu\text{m}$ above the surface. The DSCS is evaluated in the azimuthal plane $\varphi = 0^\circ$. The wavelength of the incident wave is $\lambda = 0.6328 \mu\text{m}$, and the excitation light wave has an inclination from the normal of 60° . The curves correspond to parallel and perpendicular incident light polarizations, and are computed with the T-matrix method and the DSM.

Then, after defining the elementary fields of electric and magnetic multipoles

$$\begin{pmatrix} \mathbf{E}_{mn}^{e,t}(k_t, \mathbf{r}) \\ \mathbf{H}_{mn}^{e,t}(k_t, \mathbf{r}) \end{pmatrix} = \begin{pmatrix} j/k\varepsilon_t \mu_t \nabla \times \nabla \times \mathbf{A}_{mn}^{e,t}(\mathbf{r}) \\ 1/\mu_t \nabla \times \mathbf{A}_{mn}^{e,t}(\mathbf{r}) \end{pmatrix} \quad (23)$$

$$\begin{pmatrix} \mathbf{E}_{mn}^{h,t}(k_t, \mathbf{r}) \\ \mathbf{H}_{mn}^{h,t}(k_t, \mathbf{r}) \end{pmatrix} = \begin{pmatrix} -1/\varepsilon_t \nabla \times \mathbf{A}_{mn}^{h,t}(\mathbf{r}) \\ j/k\varepsilon_t \mu_t \nabla \times \nabla \times \mathbf{A}_{mn}^{h,t}(\mathbf{r}) \end{pmatrix} \quad (24)$$

and the elementary fields of electric dipoles

$$\begin{pmatrix} \mathbf{E}_n^{e,t}(k_t, \mathbf{r}) \\ \mathbf{H}_n^{e,t}(k_t, \mathbf{r}) \end{pmatrix} = \begin{pmatrix} j/k\varepsilon_t \mu_t \nabla \times \nabla \times \mathbf{A}_{0n}^{e,t}(\mathbf{r}) \\ 1/\mu_t \nabla \times \mathbf{A}_{0n}^{e,t}(\mathbf{r}) \end{pmatrix} \quad (25)$$

where $t = s, i$, we can represent the approximate solution of the scattering problem for P polarized field as

$$\begin{pmatrix} \mathbf{E}_t^{\mathcal{N}}(\mathbf{r}) \\ \mathbf{H}_t^{\mathcal{N}}(\mathbf{r}) \end{pmatrix} = \sum_{n=1}^N \sum_{m=0}^M \left[e_{mn,t}^{\mathcal{N}} \begin{pmatrix} \mathbf{E}_{mn}^{e,t}(k_t, \mathbf{r}) \\ \mathbf{H}_{mn}^{e,t}(k_t, \mathbf{r}) \end{pmatrix} + f_{mn,t}^{\mathcal{N}} \begin{pmatrix} \mathbf{E}_{mn}^{h,t}(k_t, \mathbf{r}) \\ \mathbf{H}_{mn}^{h,t}(k_t, \mathbf{r}) \end{pmatrix} \right] + \sum_{n=1}^N r_{n,t}^{\mathcal{N}} \begin{pmatrix} \mathbf{E}_n^{e,t}(k_t, \mathbf{r}) \\ \mathbf{H}_n^{e,t}(k_t, \mathbf{r}) \end{pmatrix}. \quad (26)$$

Here, \mathcal{N} is a complex index incorporating M and N .

As it was already mentioned, the last representation for the electromagnetic field satisfies all conditions of the scattering problem under examination except the transmission conditions at the particle surface. These conditions have to be used to determine the DS amplitudes. There are various schemes for amplitude determination. A more reliable technique is the point-matching of the Fourier harmonics at the particle surface. In this case, stable results can be obtained by using an over-determined system of linear equations [11]. After DS amplitude determination one can calculate the scattering diagram using asymptotic expressions of Weyl-Sommerfeld integrals [7].

3. Numerical simulations

The goal of our numerical experiments is to investigate the convergence of the T-matrix approach by choosing the DSM as reference. We compute the differential scattering cross section (DSCS) for oblate polystyrene particles with a refractive index of 1.59 deposited on a silicon substrate with a refractive index of $3.88 + 0.02j$. Assuming the incident field to have

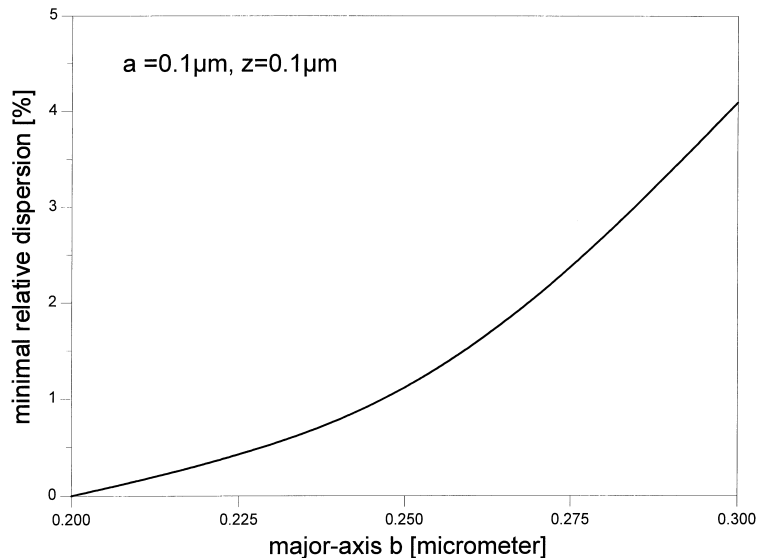


Fig. 6. Minimal relative dispersion σ_r of the differential scattering cross section (DSCS) at a scattering angle of 0° as a function of the major-axis of the spheroids b . The minor-axis of the spheroids is $a = 0.1 \mu\text{m}$ and the axial distance is $z_0 = 0.1 \mu\text{m}$. The incident light is a p-polarized plane wave with an inclination from the normal of 0° .

unit amplitude we evaluate the DSCS in the azimuthal plane $\varphi = 0^\circ$, which corresponds to the plane of incidence. The wavelength of the incident wave is chosen to be $\lambda = 0.6328 \mu\text{m}$.

First, we consider an oblate spheroid with semiaxes $a = 0.1 \mu\text{m}$ and $b = 0.3 \mu\text{m}$, and compute the DSCS by varying the axial distance z_0 from $0.1 \mu\text{m}$ to $0.3 \mu\text{m}$. In the case $z_0 = 0.1 \mu\text{m}$ the particle is situated on the substrate, while the case $z_0 = 0.3 \mu\text{m}$ corresponds to the situation in which the sphere circumscribing the particle is tangent to the substrate. Note that the focal distance is about $c = 0.28 \mu\text{m}$. Since the convergence over the truncation index N is decisive for the convergence of the T-matrix method we consider an incident p-polarized plane wave at normal incidence. The numerical simulations show that the T-matrix method does not converge when $z_0 < c$, and the method becomes more unstable when the axial distance z_0 decreases. This is demonstrated in Fig. 2. Here we plot for $z_0 = 0.225 \mu\text{m}$, $z_0 = 0.15 \mu\text{m}$, and $z_0 = 0.1 \mu\text{m}$ the relative error of the DSCS at a scattering angle of 0° as a function of the truncation index N . Our numerical analysis reveals that for each axial distance z_0 there exists a certain domain of variation of the truncation index $[N_{\min}, N_{\max}]$ characterized by

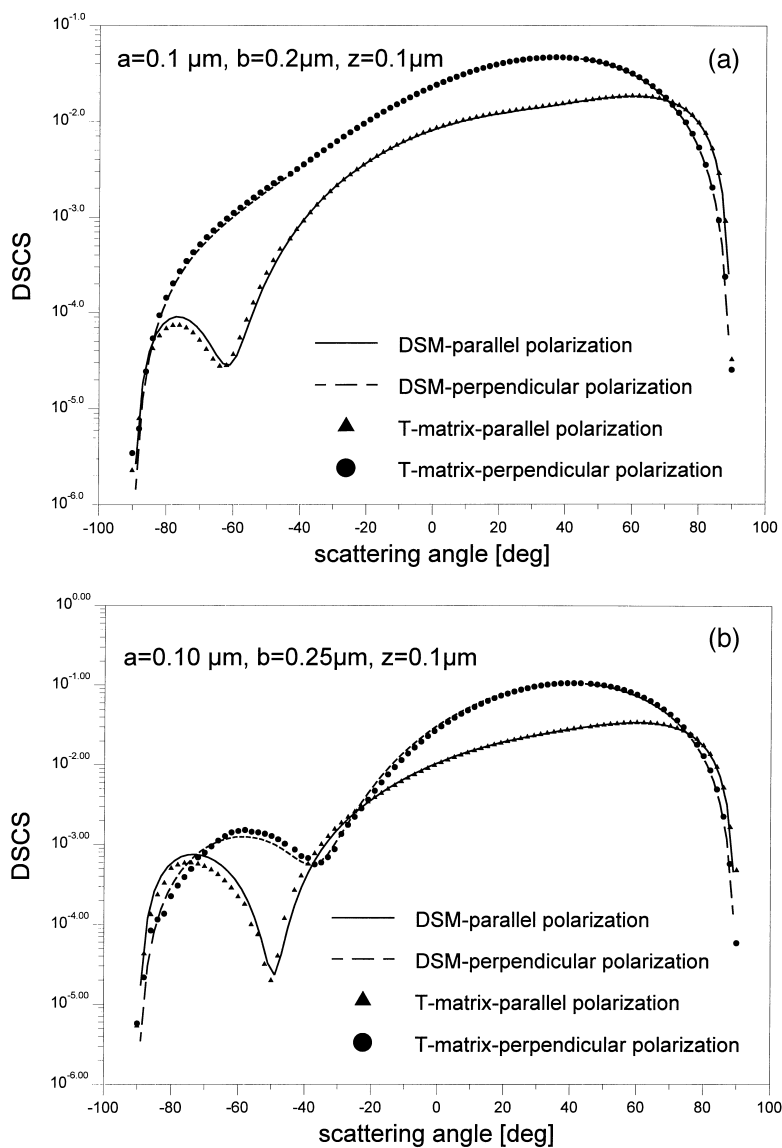


Fig. 7. Differential scattering cross section (DSCS) for oblate spheroids with semiaxes $a = 0.1 \mu\text{m}$ and (a) $b = 0.2 \mu\text{m}$, and (b) $b = 0.25 \mu\text{m}$ situated on the surface. The DSCS is evaluated in the azimuthal plane $\varphi = 0^\circ$. The wavelength of the incident wave is $\lambda = 0.6328 \mu\text{m}$, and the excitation light wave has an inclination from the normal of 60° . The curves correspond to parallel and perpendicular incident light polarizations, and are computed with the T-matrix method and the DSM.

small oscillations of the DSCS. Actually, for $N > N_{\max}$ the scattered field solution deteriorates significantly. In order to quantify the oscillations of the scattered field solution we define the relative dispersion σ_r of the DSCS by

$$\sigma_r = \frac{\sigma}{m} \times 100 \quad [\%],$$

where σ and m are the standard deviation and the mean value of the DSCS computed for a sequence of 10 consecutive values of the truncation index in the domain $[N_{\min}, N_{\max}]$. Fig. 3 shows the relative dispersion σ_r for $z_0 = 0.1 \mu\text{m}$. The curve illustrates that there exists a sequence of truncation indices characterized by a minimal relative dispersion. In Fig. 4 we plot the minimal relative dispersion σ_r of the DSCS at a scattering angle of 0° as a function of the axial distance z_0 . The results show that σ_r increases from 0 to 4.2% when the axial distance z_0 decreases from $0.3 \mu\text{m}$ to $0.1 \mu\text{m}$.

Even we do not have at our disposal a convergent solution to the scattering problem we can define a so-called optimal scattered field solution by choosing an appropriate value for the truncation index N . For this purpose we consider the sequence (consisting of 10 consecutive values of the truncation index) with the minimal relative dispersion. Then, we define the optimal scattered field solution as the solution corresponding to that value of the truncation index N which provides a minimal relative error of the DSCS with respect to the mean selection. For this value of the truncation index we compute the DSCS for a plane wave excitation having an inclination from the normal of 60° . The results are plotted in Fig. 5 for $z_0 = 0.2 \mu\text{m}$ and $z_0 = 0.1 \mu\text{m}$. The curves correspond to parallel and perpendicular incident light polarizations, and are computed with the T-matrix method and the DSM. The values of the truncation index are $N = 23$ in the case $z_0 = 0.2 \mu\text{m}$, and $N = 32$ in the case $z_0 = 0.1 \mu\text{m}$. The results show that the discrepancies between the scattering curves are not significant in the first case, but are pronounced in the second one.

Next, we consider oblate spheroids with the same minor-axis, $a = 0.1 \mu\text{m}$, situated on the interface. The aim of these numerical experiments is to investigate the convergence of the T-matrix method when the semiaxis b increases from $0.2 \mu\text{m}$ to $0.3 \mu\text{m}$. It is readily seen that in all cases under consideration the spheres enclosing the scattered field singularities (the radius of these spheres varies from $0.17 \mu\text{m}$ to $0.28 \mu\text{m}$) do intersect. Conversely, instability and convergence problems should occur by increasing b . The dependence of the minimal relative dispersion on the major-axis of the spheroid is plotted in Fig. 6. It was surprising to find that for $b = 0.2 \mu\text{m}$ the T-matrix method solution converges. The explanation lies in the fact that when the semiaxis b and the spheroid eccentricity $\varepsilon = b/a$ are small the number of terms needed in the expansions (3) and (4) is small. In this case the matrix equation includes Hankel functions of low order which in turns leads to a stable numerical algorithm. Fig. 7 shows the scattering patterns for oblate spheroids with $b = 0.2 \mu\text{m}$ and $b = 0.25 \mu\text{m}$ by considering a plane wave incidence of 60° . As before, the curves correspond to the optimal solution with respect to the truncation index N . The values of the truncation index are $N = 15$ in the case $b = 0.2 \mu\text{m}$, and $N = 22$ in the case $b = 0.25 \mu\text{m}$. The agreement with the DSM is good in the first case, and quite satisfactory in the second one.

From the above analysis we may conclude that we are not able to achieve convergence when the geometrical constraint of the T-matrix method is violated. The oscillations of the scattered field solution become more pronounced by increasing the particle eccentricity and by decreasing the distance from the substrate. For practical applications a simple possibility for finding the optimal solution is at our disposal. Essentially, we have to compute the DSCS for normal incidence and different values of the truncation index N . Then, we have to select from sequences having the same number of values, that sequence for which the dispersion parameter is minimal, and finally, we have to choose that value of the truncation index N which guarantees a minimal relative error of the DSCS with respect to the mean selection.

4. Conclusions

The range of validity of the T-matrix approach for analyzing the scattering light from particles deposited on a plane surface is investigated. Numerical experiments are performed for oblate spheroids situated on the substrate or above the substrate by choosing a model based on the discrete source method as reference. The analysis shows that convergence problems occur when the sphere enclosing the singularities of the scattered field intersects the interface. Consequently, the scattered field solution oscillates. An optimal solution with respect to the truncation index N can be defined by analyzing statistically the DSCS for normal incidence. It was found that if the relative dispersion of the DSCS is sufficiently small (for example, $\sigma_r < 1.5\%$), the optimal solution computed by the T-matrix approach does not differ significantly from the exact solution computed by the DSM.

Acknowledgements

This research was supported by the Volkswagen-Stiftung under grant I/70984.

References

- [1] P.A. Bobbert, J. Vlieger, *Physica A* 137 (1986) 209.
- [2] G. Videen, *J. Opt. Soc. Am. A* 8 (1991) 483.
- [3] G. Videen, *J. Opt. Soc. Am. A* 10 (1993) 110.
- [4] G. Videen, *J. Opt. Soc. Am. A* 10 (1993) 118.
- [5] M.A. Taubenblatt, T.K. Tran, *J. Opt. Soc. Am. A* 10 (1993) 912.
- [6] B.M. Nebeker, G.W. Starr, E.D. Hirleman, Light scattering from patterned surfaces, particles on surfaces, in: J.K. Lowell, R.T. Chen, J.P. Mathur (Eds.), *Optical Characterization Techniques for High Performance Microelectronic Device Manufacturing II*, Proc. SPIE 2638 (1995) 274.
- [7] Y. Eremin, N. Orlov, *Appl. Optics* 35 (1996) 6599.
- [8] T. Wriedt, A. Doicu, *Optics Comm.* 152 (1998) 376.
- [9] P.C. Waterman, *J. Acoust. Soc. Am.* 45 (1969) 1417.
- [10] P.W. Barber, S.C. Hill, *Light Scattering by Particles: Computational Methods*, World Scientific, Singapore, 1990.
- [11] Yu.A. Eremin, A.G. Sveshnikov, *Electromagnetics* 13 (1993) 1.